Journal of Power Sources 195 (2010) 1171–1176

Contents lists available at ScienceDirect

Journal of Power Sources

journal homepage: www.elsevier.com/locate/jpowsour

Short communication

Proton exchange membrane fuel cell degradation under close to open-circuit conditions Part I: In situ diagnosis

Jinfeng Wu[a], Xiao-Zi Yuan[a], Jonathan J. Martin[a], Haijiang Wang[a,*], Daijun Yang[b], Jinli Qiao[b], Jianxin Ma[b]

[a] Institute for Fuel Cell Innovation, National Research Council of Canada, 4250 Wesbrook Mall, Vancouver, B.C., Canada V6T 1W5
[b] Clean Energy Automotive Engineering Center, Tongji University (Jiading Campus), 4800 Caoan Road, Shanghai 201804, China

ARTICLE INFO

Article history:
Received 20 July 2009
Received in revised form 29 August 2009
Accepted 31 August 2009
Available online 6 September 2009

Keywords:
Proton exchange membrane fuel cell
Stack
In situ
Durability
Close to open-circuit conditions
Degradation mechanism

ABSTRACT

Durability of polymer exchange membrane (PEM) fuel cells under a wide range of operational conditions has been generally identified as one of the top technical gaps that need to be overcome for the acceptance of this fuel cell technology as a commercially viable power source, especially for automotive and portable applications. In this study, a 1200 h lifetime test was conducted with a six-cell PEM fuel cell stack under close to open-circuit conditions. In situ measurements of the hydrogen crossover rate through the membrane, high frequency resistance and electrochemically active surface area of each single cell, in combination with cell polarization curves, were used to investigate the degradation mechanisms. Direct gas mass spectrometry of the cathode exhaust gas indicated the formation of HF, H_2O_2 and CO_2 during the durability testing. The overall cell degradation rate under this accelerated stress testing is approximately 0.128 mV h^{-1}. The cell degradation rate for the first 800 h is much lower than that after 800 h, which may result from the dominance of different degradation mechanisms. For the first period, the degradation of fuel cell performance was mainly attributed to catalyst decay, while the subsequent dramatic degradation is likely caused by membrane failure.

1. Introduction

In recent years, with potential to replace the internal combustion engine in light-duty vehicles, proton exchange membrane (PEM) fuel cells have attracted much attention due to various advantages, such as fast-start capability and low temperature operation. However, PEM fuel cell durability, especially under a wide range of operational conditions, is still one of the current limitations preventing its wide scale commercialization as a practical power source. More thorough studies on components and the analysis of system failure modes are currently imperative due to the integrated nature of the issues. A fuel cell stack is a complicated system comprised of various components for which the degradation mechanisms, component interactions, and effects of operating conditions need to be fully understood prior to commercialization.

However, so far only a relatively small number of studies aiming at real PEM fuel cell lifetimes have been conducted, owing to the high costs and prolonged testing periods required. Meanwhile, various ex situ accelerated tests have been proposed and implemented to explore degradation mechanisms of individual components in PEM fuel cells. For example, Fenton's test, using a H_2O_2 solution containing a trace amount of Fe^{2+}, has been commonly employed as an ex situ method to analyze the chemical degradation of membranes [1,2]. Also, the stress–strain test [3] and relative humidity (RH) cycling [4] have always been selected as accelerated means for understanding the mechanical degradation of membranes.

The research progresses on PEM fuel cell durability and degradation have been reviewed from many different perspectives. The review of Borup et al. [5] concentrated on the fundamental aspects of PEM fuel cell degradation mechanisms. Shao et al. [6] and Zhang et al. [7] paid attention to the material challenges to developing durable high temperature PEM fuel cells, including electrocatalysts, carbon supports, membranes, polymers, and bipolar plates. In more recent reviews, Zhang et al. [8] and de Bruijn et al. [9] introduced in detail the methods to accelerate performance decay and component damage from both chemical and mechanical perspectives. While in our recent review [10], the existing strategies for improving the lifetime of the fuel cell components were summarized.

In order to increase sample throughput and reduce the experimental time required, different undesirable operating conditions

* Corresponding author. Tel.: +1 604 221 3038; fax: +1 604 221 3001.
E-mail address: haijiang.wang@nrc-cnrc.gc.ca (H. Wang).

0378-7753/$ – see front matter.
doi:10.1016/j.jpowsour.2009.08.095

have been utilized as the in situ accelerated stressors, such as loading cycling [11,12], start–stop cycles [13], low relative humidity (RH) [14,15] or RH cycling [4], freeze–thaw cycles [16] as well as fuel [17,18] or air starvation [19]. Open-circuit (OC) operation has also been recognized as an effective stressor for accelerated testing in PEM fuel cell durability studies and the accelerated effects of OC operation on the degradation of PEM fuel cell components including PEM and catalyst layer have been investigated [20–24]. Whereas, little attention has been paid to the performance degradation of a PEM fuel cell under close to OC conditions when only idle auxiliary load power is drawn from the power supply with a relatively high fuel cell potential of around 0.9 V [25]. The durability and reliability under idle conditions is a vital and practical factor for the acceptance of the fuel cell technology as a commercially viable power supply, especially for automotive and portable applications. With regard to vehicles, for example, the idle time may amount to several thousand hours over the lifetime of the fuel cell [25].

In this study, a 1200 h lifetime test with a six-cell PEM fuel cell stack was conducted under close to OC conditions. After every 300 h of testing, one cell was taken out of the stack for further analysis of the membrane electrode assembly's (MEA's) degradation. During the testing, various in situ electrochemical and chemical diagnostic tools were utilized, such as polarization curves, cyclic voltammetry (CV), linear sweep voltammetry (LSV), electrochemical impedance spectroscopy (EIS) and direct gas mass spectrometry (DGMS). As a result, the overall degradation rate under this accelerated stressor could be obtained and the change in fuel cell properties with time, such as electrochemically active surface area (ECA), hydrogen crossover rate through the membrane, and ohmic resistance could be measured. Based on the experimental data, the degradation mechanisms of fuel cells under close to OC conditions were explored.

2. Experimental

2.1. Fuel cell materials and testing apparatus

A six-cell Tandem® TP50 fuel cell stack (Tandem Tech. Ltd., Canada) was utilized for performing the PEM fuel cell degradation testing under close to OC conditions. For each single cell, the active area was 50 cm^2 with a single serpentine channel for the anode flow field and dual parallel serpentine channels for the cathode flow field. The Sigracet® gas diffusion media, 25 BC and 25 DC with microporous layers (SGL Carbon, Germany), were used as the cathode and anode gas diffusion layers (GDL), respectively. The MEA was assembled by sandwiching Gore™ PRIMEA® series 57 catalyst coated membranes (CCMs), with 0.4 $mg_{Pt}\,cm^{-2}$ Pt/C loading, between of the anode and cathode GDLs. Polyimide film with silicon adhesive on one side was used as the sub-gasket to protect the edges of the CCM. Homemade die cutters were used to cut the GDLs, CCMs and sub-gaskets and the polyimide sub-gaskets were bonded to both sides of the CCM, forming an active area of 50 cm^2.

The durability testing under close to OC conditions was carried out on a 500 W Fuelcon® test station (Fuelcon Inc., Germany). During the testing, the six-cell fuel cell stack was operated at a constant current of 0.5 A (10 mA cm^{-2}). This relatively low current density was chosen in this experiment as a consequence of the high average cell voltage of around 0.9 V at the beginning of life (BOL). The fuel cell stack temperature was kept at 70 °C and air and hydrogen were fully humidified at 70 °C prior to their delivery into the fuel cell. The flow rates for air and hydrogen were set at 2.0 and 0.5 standard liters per minute (SLPM), respectively. After every 300 h of operation, one cell was randomly taken out of the stack for further ex situ analysis and the remaining cells continued the degradation testing under close to OC conditions.

2.2. In situ electrochemical and chemical measurements

Besides the fuel cell performance test, before and after every 100 h of operation, CV, LSV, and EIS measurements were conducted to determine the ECA of the cathode electrode, the hydrogen crossover rate, and fuel cell internal resistance, respectively. During the polarization curve measurement, the stack was operated at 70 °C and fully humidified air and hydrogen were supplied to the stack at stoichiometries of 2.5 and 1.5, respectively. When the CV, LSV, and EIS measurements were performed, the testing stack was also kept at 70 °C and fully humidified hydrogen and nitrogen were introduced to the anode and cathode at constant flow rates of 3.0 and 3.3 SLPM, respectively. For the CV test, a Solartron 1287 electrochemical interface (Solartron Instrument, US) was utilized and the voltage sweep was controlled in a range of 0.04–1.0 V with a sweep rate of 20 mV s^{-1}. For the LSV measurement, the potential of the cathode was linearly swept from 0.05 to 0.4 V against the anode at a rate of 1 mV s^{-1}. The EIS measurement was also carried out at open-circuit potential using a Solartron 1260 frequency response analyzer (Solartron Instrument, US) together with the Solartron 1287 electrochemical interface. A small alternating voltage perturbation (5 mV) was imposed on the cell over a range of frequencies from 3000 to 10 Hz and the real component of the resulting impedance represented the ohmic resistance of the cell. During the durability testing, the exhaust air was characterized by an on-line HPR-20 quadrupole mass spectrometer (Hiden Analytical, England) in 30 min intervals to monitor the possible degradation products.

3. Results and discussion

3.1. Performance degradation of the stack

The polarization curve of each cell prior to durability testing and the average performance of six cells are depicted in Fig. 1. The BOL performances of the six single cells were quite close. As shown in Fig. 1, the performance difference between the six cells is less than 1.0% in the range of low current densities (less than 500 mA cm^{-2}), and the difference is only 0.67% when the stack current density was controlled at 10 mA cm^{-2}. In the range of high current densities, the differences increase slightly, which is likely attributed to the maldistribution of the reactants among the different cells in the stack.

The voltage changes of the cells with time under close to OC conditions are presented in Fig. 2. Interruptions during the testing resulted from unexpected shutdowns of the power or gas supply in the lab. After 1200 h of operation, the testing was terminated owing

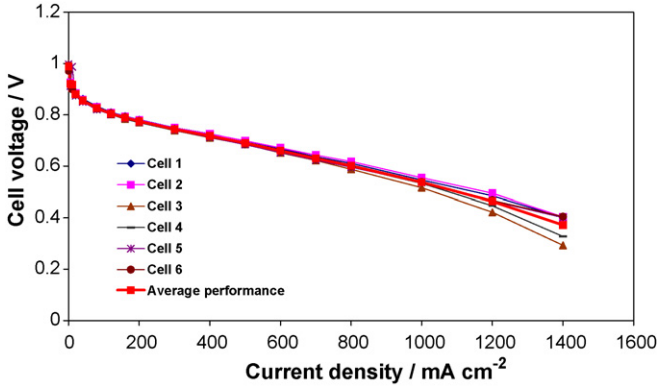

Fig. 1. Polarization curves of each cell in the stack prior to the degradation test: cell temperature at 70 °C; humidifier temperature of air/hydrogen at 70/70 °C; gas pressure of air/hydrogen at atmosphere; stoichiometries of air/hydrogen at 2.5/1.5.

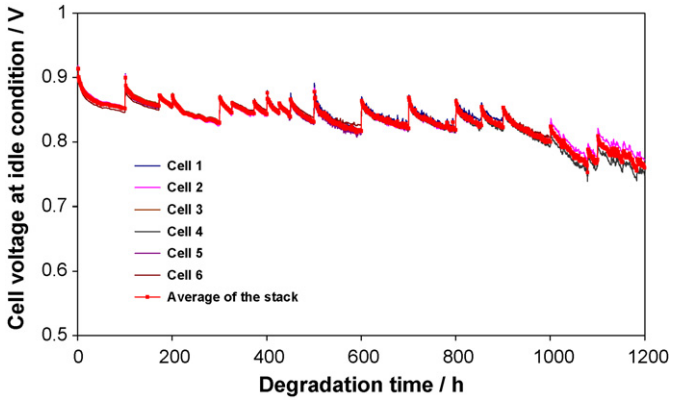

Fig. 2. The change of each cell voltage and the average voltage of the stack with time under close to OC conditions: cell temperature at 70 °C; humidifier temperature of air/hydrogen at 70/70 °C; gas pressure of air/hydrogen at atmosphere; flow rates of air/hydrogen at 2.0/0.5 SLPM.

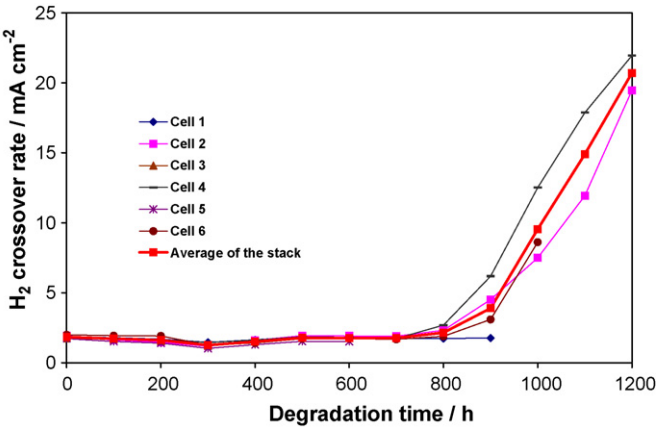

Fig. 4. The change of hydrogen crossover rate through the membrane of each cell with time of 1200 h: the operating conditions are the same as those in Fig. 3.

to the low performance and elevated hydrogen crossover rate through the MEAs. The overall degradation rate for the stack under close to OC conditions is 0.128 mV h^{-1} and it is worth noting that the degradation rate from the first 800 h was much lower than that after 800 h, as depicted in Fig. 2. During the first 800 h of operation, the average performance of the stack slowly decreased from 0.914 to 0.819 V and the degradation rate was approximately 0.119 mV h^{-1}. While after about 800 h running, an accelerated decrease from 0.864 to 0.760 V in 400 h was observed, and the voltage decay rate reached 0.260 mV h^{-1}.

3.2. Electrochemical and chemical characterization during degradation testing

CV measurements were carried out intermittently with each cell of the stack and, accordingly, the ECA of each cathode catalyst layer was obtained based on the hydrogen desorption peak on CV curves. The changes in the ECA of each cell and the average ECA of the stack with time are demonstrated in Fig. 3. It can be seen that the ECA changes for all the cells follow a similar trend and under our operating conditions, the average ECA of the stack decreases slowly from 0.037 C cm^{-2} at BOL to 0.021 C cm^{-2} at 800 h. Several reasons may account for this gradual decrease in the ECA of the catalyst layer. The corrosion of the catalyst carbon support can decrease the number of sites available to anchor the catalyst, leading to aggregation of catalyst particles and a reduction of the ECA, which is confirmed by the DGMS result below. As for this study, carbon corrosion will be much more pronounced as a result of the relatively high cell voltage. In addition to the carbon support corrosion, the coarsening of the catalyst due to particle movement and coalescence on the carbon support can also cause the catalytically active surface area to decrease during durability testing [26,27]. Finally, the slow dissolution of the Nafion® resin in the catalyst layer during long-term contact with water is unavoidable. The fluoride emission rate (FER) from effluent water has been considered evidence of Nafion® degradation [24]. However, this process is difficult to distinguish from the degradation of PEM due to its integrity. The loss of the polymer resin may cause some Pt catalyst to be unavailable for electrochemical reaction and consequently reduce the ECA of the catalyst layer. A speedy decay from 0.021 to 0.002 C cm^{-2} in the subsequent 400 h can be seen in Fig. 3, which is likely ascribed to the hydrogen crossover and membrane degradation, as described below in the LSV analysis.

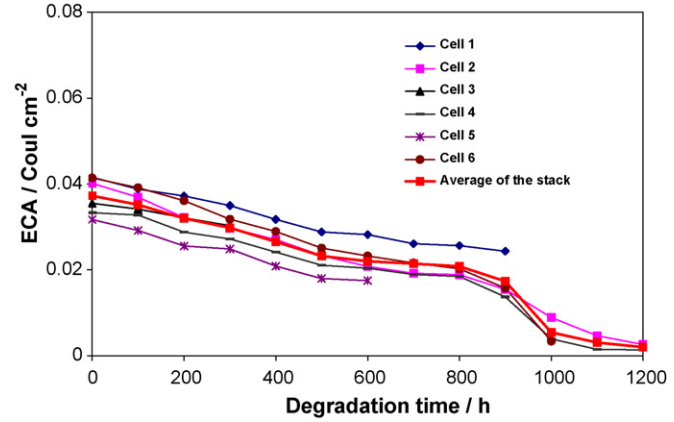

Fig. 3. The ECA change of each cell with time of 1200 h: cell temperature at 70 °C; humidifier temperature of nitrogen/hydrogen at 70/70 °C; flow rate of nitrogen/hydrogen at 3.3/3.0 SLPM.

At every 100 h, an LSV measurement was conducted with each cell and the hydrogen crossover rate was determined by the hydrogen oxidation current density obtained in the 300–350 mV range of the voltammogram. In this voltage range, the current density is limited by the direct oxidation of permeated hydrogen across the membrane at the cathode, which is free from the effects of hydrogen adsorption/desorption on catalyst [28]. The change of hydrogen crossover current density through the membrane with time is demonstrated in Fig. 4. During the fuel cell degradation, the average hydrogen crossover current density of the stack slightly increases from 1.84 mA cm^{-2} at BOL to 2.15 mA cm^{-2} at 800 h. Subsequently, the average hydrogen crossover rate significantly increases to 9.54 mA cm^{-2} at 1000 h and ultimately to 20.71 mA cm^{-2} at 1200 h. After 1000 h of degradation, cell 6 had to be taken out of the stack due to its abnormally low performance, which could be ascribed to the extremely low ECA and high hydrogen crossover rate. As shown in Figs. 3 and 4, the ECA of its catalyst layer is quite low (0.0034 C cm^{-2}) and hydrogen crossover current density is quite high (8.62 mA cm^{-2}) at 1000 h.

EIS of each cell was monitored periodically during the degradation testing and its change with time is shown in Fig. 5. It can be seen that there is a slight increase in average ohmic resistance from 31.3 mΩ at the beginning to 35.5 mΩ at 1200 h, which implies that severe delamination or collapse did not occur in the MEAs during the 1200 total operating hours. As for the impedance spectra of a PEM fuel cell, the real component of the high frequency end of the kinetic arc is mainly due to the electronic and ionic resistances of the membrane. Additional contributions come from catalyst layers, gas diffusion layers, and current collectors. The chemical degrada-

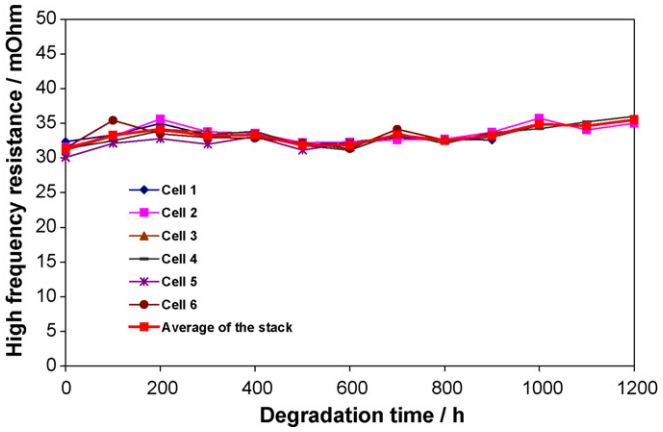

Fig. 5. The change of high frequency resistance of each cell with time of 1200 h: the operating conditions are the same as those in Fig. 3.

tion of the electrolyte membrane can result in membrane thinning, as described below in Section 3.3, which not only leads to a lower ohmic resistance but also correspondingly leads to a decrease in ionic conductivity. Moreover, carbon corrosion due to a combination of high cell voltage and prolonged operation may play a role in the total resistance increase.

In situ DGMS analysis was carried out for the cathode exhaust gas every 30 min in order to identify the gas components resulting from the degradation processes. The final results showed that the gas composition was not consistent during the testing and Fig. 6a and b obtained at 539 and 1052 h, respectively, were selected. The

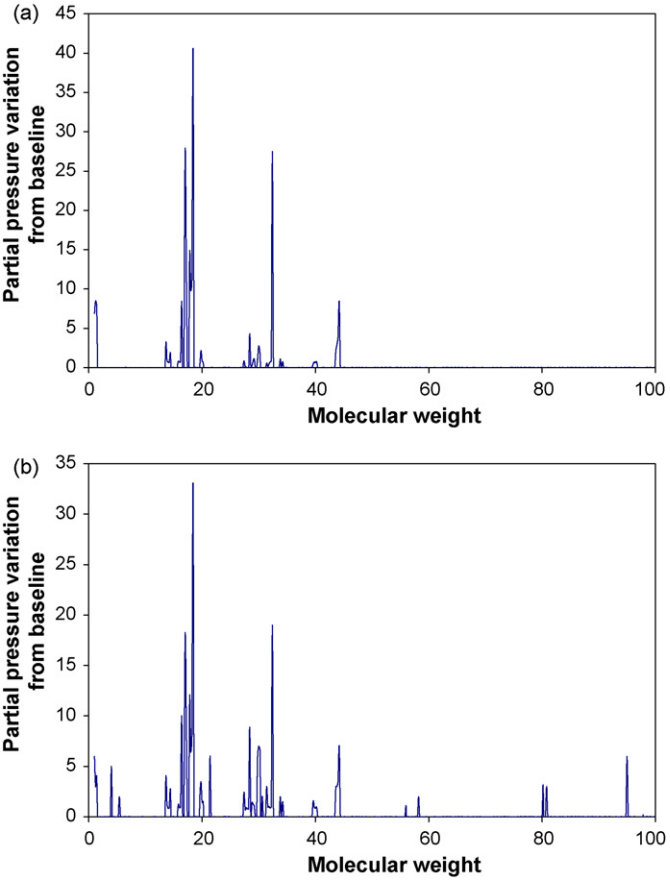

Fig. 6. The exhaust gas components obtained at (a) 539 h and (b) 1052 h, respectively: the operating conditions are the same as those in Fig. 2.

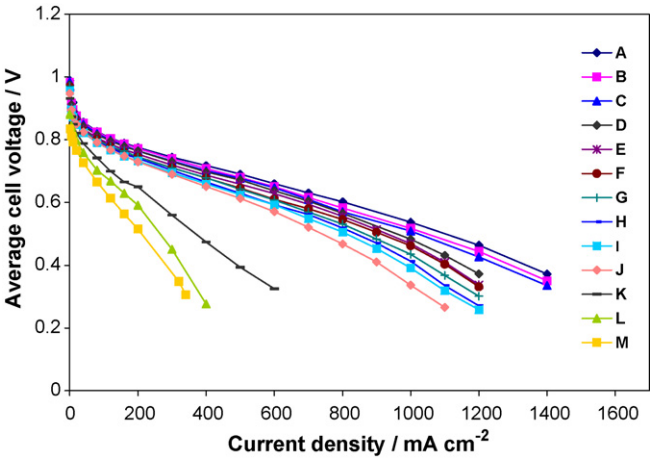

Fig. 7. Average performance change of the PEM fuel cell stack with time: (A) BOL, (B) 100 h, (C) 200 h, (D) 300 h, (E) 400 h, (F) 500 h, (G) 600 h, (H) 700 h, (I) 800 h, (J) 900 h, (K) 1000 h, (L) 1100 h, and (M) 1200 h. The operating conditions are the same as those in Fig. 1.

baseline was also acquired by DGMS, keeping the same air flow rate and relative humidity as the degradation testing but bypassing the fuel cell stack. As shown in Fig. 6a and b, the molecular weights of 20, 28, 34 and 44 were detected, which can be assigned to HF, CO or N_2, H_2O_2 and CO_2, respectively [29]. CO_2 is an evidence of carbon corrosion and the presence of H_2O_2 can be ascribed to the trigger of membrane degradation. In the presence of impurity cations such as Fe^{2+} and Cu^{2+} ions, H_2O_2 decomposes to peroxide (HO·) and hydroperoxide (HOO·) radicals, and these radicals will attack the susceptible electrolyte polymer with residual H-containing terminal bonds at the end group sites and initiate membrane decomposition [1]. The chemical degradation strongly accelerates membrane thinning and performance decay of a PEM fuel cell. Compared with Fig. 6a obtained at 539 h, Fig. 6b shows more complicated gas components such as H_2SO_3 (molecular weight of 82), which can be attributed to the elevated temperature caused by the highly exothermic combustion of hydrogen and air, resulting in thermal degradation of the membranes, polymer resin and polytetrafluoroethylene (PTFE) in the MEAs.

3.3. Exploration of the degradation mechanisms

The accelerated degradation after 800 h of operation is pronounced when the average performance change of the PEM fuel cell stack is demonstrated over time, as shown in Figs. 7 and 8 g. For the first 800 h, the average performance decreases gradually with time, while it deteriorates sharply for the following 400 h until the catastrophic failure of the fuel cell stack at 1200 h. It is worth noting that even for the first 800 h, the degradation rate of each cell at different cell voltages is clearly different, as shown in Fig. 8. As for the open-circuit voltage (OCV), it can be observed that there is a slight decrease from 0.989 to 0.956 V in the first stage of operation. The OCV at BOL was 0.989 V, which is a little lower than the theoretical potential (1.191 V at 70 °C) [30]. The difference in OCV is caused mainly by two factors: one is the mixed potential of the Pt/PtO catalyst surface, and the other is hydrogen crossover [31]. The reaction of the oxide film formation on the Pt catalyst surface is reversible and hence it is not an essential degradation phenomenon [32]. Since the operating conditions were fixed during the degradation testing, the loss in OCV due to the partial oxidation of Pt catalyst should have been stable and had no appreciable influence on OCV change over time. Consequently, the slight reduction in OCV in the first 800 h can be attributed to the increased hydrogen crossover current density from 1.84 to 2.15 mA cm^{-2}, as shown in

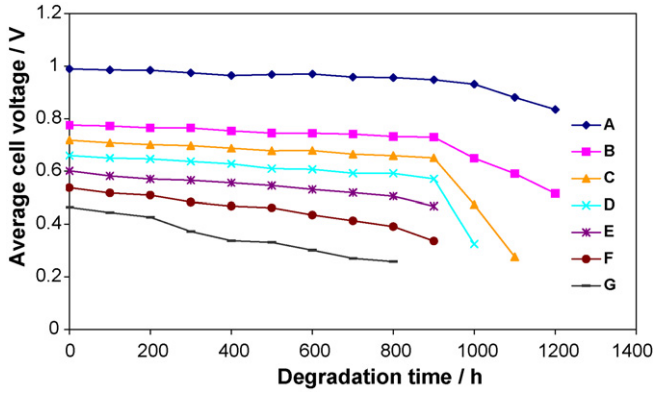

Fig. 8. Average cell voltage change with time at different current densities: (A) 0 mA cm^{-2}, (B) 200 mA cm^{-2}, (C) 400 mA cm^{-2}, (D) 600 mA cm^{-2}, (E) 800 mA cm^{-2}, (F) 1000 mA cm^{-2}, and (G) 1200 mA cm^{-2}. The operating conditions are the same as those in Fig. 1.

Fig. 4. The hydrogen that crossed over could react with oxygen to produce a corresponding cathodic current density, resulting in a depression of the cathode potential and elevated cathode overpotential. However, the resulting performance decay is more drastic at higher average cell current densities. For example, a dramatic drop can be observed from 0.464 to 0.258 V at 1200 mA cm^{-2} in the first 800 h, which can be ascribed to the decrease of the ECA of the catalyst layer, as demonstrated in Fig. 3. In the range of high current densities, the Pt catalyst cannot provide enough active sites for the electrochemical reaction due to the loss of ECA. While, for the low current densities, the needed active sites of the Pt catalyst are much lower than those at high current densities, and therefore the performance decay rate is lower.

As described above, the chemical reaction on the anode and cathode catalysts due to gas crossover can produce HO· and HOO· radicals, which are generally believed to be responsible for chemical degradation of the membrane [33,34]. Further investigation has also revealed that the generation of these radicals, as well as the chemical degradation of the membrane, is accelerated when the fuel cell is operated under high cell voltage [15]. The chemical degradation will cause the thinning of the membrane, which in turn results in higher gas crossover rate and more severe chemical degradation. During the first 800 h of degradation, the chemical degradation of the membrane is not obvious due to the extremely low gas crossover rate. However, as the hydrogen crossover rate increases, more reactant gases will penetrate into their respective reverse electrodes and the mixed potentials in both cathode and anode sides will definitely decrease the cell performance. Meanwhile, highly exothermic direct combustion of H_2 and O_2 occurs on the catalyst surface and results in hotspots. The coarsening of the catalyst at these hotspots will be greatly accelerated, which consequently leads to the dramatic loss in ECA of the catalyst layer after 800 h of degradation, as demonstrated in Fig. 3. More seriously, the hotspots may result in local pinholes and perforations through the membrane, and if this happens, a destructive cycle of increasing gas crossover and pinhole production will be then established, which undoubtedly accelerates thermal degradation of the membrane and the entire stack. As depicted in Fig. 4, the hydrogen crossover rate starts to accelerate after about 800 h, which is most likely caused by the formation of pinholes or perforations and eventually results in the catastrophic failure of the fuel cell at 1200 h.

After 1200 h of durability testing, the six MEAs with different degradation times were finally obtained. Ex situ analyses of the degraded MEAs are under investigation. Various ex situ diagnostic tools including scanning electron microscopy (SEM), transmission electron microscopy (TEM), contact angle goniometry and infrared camera are and will be employed. The property changes of the GDLs, catalyst layers and membranes during ageing, such as contact angle, catalyst particle size, microstructure of catalyst layer, and membrane thickness will be measured. Ex situ diagnostic methods, together with in situ data, will thoroughly probe the degradation mechanisms of the PEM fuel cell under close to OC conditions.

4. Conclusions

In this study, a 1200 h lifetime test was conducted with a six-cell PEM fuel cell stack under close to OC conditions. The experimental results show that the overall cell degradation rate under this AST is approximately 0.128 mV h^{-1}. In situ electrochemical and chemical diagnostic methods, including polarization curve, cyclic voltammetry, linear sweep voltammetry, electrochemical impedance spectroscopy, and direct gas mass spectroscopy, were employed during the testing to explore the degradation mechanisms. The results show that the cell degradation rate for the first 800 h is much lower than that after 800 h, which may result from the dominance of different degradation mechanisms. The slow degradation in the first stage may be mainly related to the coarsening of the platinum catalyst and the following accelerated decay is most likely caused by the catastrophic failure of the membrane.

Acknowledgements

The authors acknowledge the NRC-MOST Joint Research Program, BCIC's ICSD Program, and NRC-Helmholtz Joint Research Program for their financial support.

References

[1] A.B. LaConti, M. Hamdan, R.C. McDonald, in: W. Vielstich, H.A. Gasteiger, A. Lamm (Eds.), Handbook of Fuel Cells: Fundamentals, Technology and Applications, vol. 3, John Wiley & Sons, Ltd., 2003, pp. 647–662.
[2] Y. Chikashige, Y. Chikyu, K. Miyatake, M. Watanabe, Macromolecules 38 (2005) 7121–7126.
[3] P. Genova-Dimitrova, B. Baradie, D. Foscallo, C. Poinsignon, J.Y. Sanchez, J. Membr. Sci. 185 (2001) 59–71.
[4] X. Huang, R. Solasi, Y. Zou, M. Feshler, K. Reifsnider, D. Condit, S. Burlatsky, T. Madden, J. Polym. Sci. 16 (2006) 2346–2357.
[5] R. Borup, J. Meyers, B. Pivovar, Y.S. Kim, R. Mukundan, N. Garland, D. Myers, M. Wilson, F. Garzon, D. Wood, P. Zelenay, K. More, K. Stroh, T. Zawodzinski, J. Boncella, J.E. McGrath, M. Inaba, K. Miyatake, M. Hori, K. Ota, Z. Ogumi, S. Miyata, A. Nishikata, Z. Siroma, Y. Uchimoto, K. Yasuda, K. Kimijima, N. Iwashita, Chem. Rev. 107 (2007) 3904–3951.
[6] Y.Y. Shao, G.P. Yin, Z.B. Wang, Y.Z. Gao, J. Power Sources 167 (2007) 235–242.
[7] J.J. Zhang, Z. Xie, J.J. Zhang, Y.H. Tang, C.J. Song, T. Navessin, Z.Q. Shi, D.T. Song, H.J. Wang, D.P. Wilkinson, Z.S. Liu, S. Holdcroft, J. Power Sources 160 (2006) 872–891.
[8] S.S. Zhang, X.Z. Yuan, H.J. Wang, W. Mérida, H. Zhu, J. Shen, S.H. Wu, J.J. Zhang, Int. J. Hydrogen Energy 34 (2009) 388–404.
[9] F.A. de Bruijn, V.A. Dam, G.J.M. Janssen, Fuel Cells 8 (2008) 3–22.
[10] J.F. Wu, X.Z. Yuan, H.J. Wang, J.J. Zhang, J. Shen, S.H. Wu, W. Mérida, J. Power Sources 108 (2008) 104–119.
[11] A. Kusoglu, A.M. Karlsson, M.H. Santare, S. Cleghorn, W.B. Johnson, J. Power Sources 161 (2006) 987–996.
[12] D. Liu, S. Case, J. Power Sources 162 (2006) 521–531.
[13] Y. Takagia, Y. Takakuwa, ECS Trans. 3 (2006) 855–860.
[14] J. Yu, T. Matsuura, Y. Yoshikawa, M.N. Islam, M. Hori, Phys. Chem. Chem. Phys. 7 (2005) 373–378.
[15] E. Endoh, S. Terazono, H. Widjaja, Y. Takimoto, Electrochem. Solid-State Lett. 7 (2004) A209–A211.
[16] R.C. McDonald, C.K. Mittelsteadt, E.L. Thompson, Fuel Cells 4 (2004) 208–213.
[17] T.R. Ralph, S. Hudson, D.P. Wilkinson, ECS Trans. 1 (2006) 67–84.
[18] A. Taniguchi, T. Akita, K. Yasuda, Y. Miyazaki, J. Power Sources 130 (2004) 42–49.
[19] S.J.C. Cleghorn, D.K. Mayfield, D.A. Moore, J.C. Moore, G. Rusch, T.W. Sherman, N.T. Sisofo, U. Beuscher, J. Power Sources 158 (2006) 446–454.
[20] Xu.F H., R. Borup, E. Brosha, F. Garzon, B. Pivovar, ECS Trans. 6 (2007) 51–62.
[21] T.A. Aarhaug, A.M. Svensson, ECS Trans. 3 (2006) 775–780.
[22] S. Kundu, M. Fowler, L. Simon, R. Abouatallah, J. Power Sources 182 (2008) 254–258.
[23] A. Ohma, S. Suga, S. Yamamoto, K. Shinohara, J. Electrochem. Soc. 154 (2007) B757–B760.

[24] S.S. Zhang, X.Z. Yuan, J.N.C. Hin, H.J. Wang, J.F. Wu, K.A. Friedrich, M. Schulze, J. Power Sources (2009), doi:10.1016/j.jpowsour.2009.08.070.
[25] M.F. Mathias, R. Makharia, H.A. Gasteiger, J.J. Conley, T.J. Fuller, G.J. Gittleman, S.S. Kocha, D.P. Miller, C.K. Mittelsteadt, T. Xie, S.G. Yan, P.T. Yu, Electrochem. Soc. Interf. 14 (2005) 24–35.
[26] K.L. More, K.S. Reeves, Microstructural characterization of PEM fuel cell MEAs, DOE Hydrogen Program, FY 2005 Progress Report.
[27] T. Akita, A. Taniguchi, J. Maekawa, Z. Siroma, K. Tanaka, M. Kohyama, K. Yasuda, J. Power Sources 159 (2006) 461–467.
[28] M. Inaba, T. Kinumoto, M. Kiriake, R. Umebayashi, A. Tasaka, Z. Ogumi, Electrochim. Acta 51 (2006) 5746–5753.
[29] K. Teranishi, K. Kawata, S. Tsushima, S. Hirai, Electrochem. Solid-State Lett. 9 (2006) A475–A477.
[30] J. Larminie, A. Dicks, Fuel Cell Systems Explained, John Wiley & Sons, Ltd., 2000, pp. 25–66.
[31] J. Zhang, Y. Tang, C. Song, J. Zhang, H. Wang, J. Power Sources 163 (2006) 532–537.
[32] M. Inaba, in: F.N. Büchi, M. Inaba, T.J. Schmidt (Eds.), Polymer Electrolyte Fuel Cell Durability, Springer Science + Business Media, 2009, pp. 51–69.
[33] F.N. Büchi, B. Gupta, O. Haas, G.G. Scherer, Electrochim. Acta 40 (1995) 345–353.
[34] H. Wang, G.A. Capuano, J. Electrochem. Soc. 145 (1998) 780–784.